

---

# Aftereffects and the representation of stereoscopic surfaces

---

Billy Lee

Department of Psychology, University of Edinburgh, 7 George Square, Edinburgh EH8 9JZ, Scotland, UK; e-mail: [B.Lee@edinburgh.ac.uk](mailto:B.Lee@edinburgh.ac.uk)

Received 16 September 1998, in revised form 27 July 1999

---

**Abstract.** The structure of human disparity representation is examined through (i) adaptation experiments and (ii) model simulations of the data. Section 3 presents results of adaptation experiments designed to illuminate the structure of human disparity representation. Section 4 presents model simulations of three different disparity representation schemes. In the experiments, participants adapted to a  $0.133 \text{ cycle deg}^{-1}$  sinusoidally corrugated surface with 10 min of arc peak-to-trough disparity. A flat test surface was briefly presented, in which the aftereffect surface was perceived. Adapt and test surfaces were placed on disparity pedestals and thus presented in front of or behind the plane of fixation. The adapt surface could be offset from the fixation plane by  $\pm 8$  to 24 min of arc. The test surface could be offset from the fixation plane by  $\pm 8$  to 48 min of arc. The depth aftereffect was measured in different disparity planes by a nulling method and 'topping-up' procedure. Aftereffect tuning functions were obtained whose bandwidths, magnitudes, and tuning depended on the disparity planes of both the adapt and test surfaces. These parameters were used to constrain the models tested in section 4. On the basis of the two studies, it is argued that the human stereoscopic system encodes spatial changes of disparity using channels localised within disparity planes. A *localised disparity-gradient model* of the human representation of disparity is proposed.

## 1 Introduction

The challenge faced by stereoscopic vision is to deliver a more or less veridical representation of the three-dimensional (3-D) world. In humans and other animals the problem is complicated by our ability to move and change our point of observation. Therefore, the stereoscopic representation must be viewpoint-invariant. It must use a representational primitive that uniquely specifies the spatial structure of the environment. Generating such a representation requires a more complex process than simply registering binocular image parallax. Simple parallax is viewpoint-variant and is therefore inadequate as a mobile primitive. Neural hardware and computation are required for the system to be tuned to a primitive that has the requisite specifications. Here, evidence is presented from (i) adaptation experiments and (ii) modelling data for a possible scheme for the organisation of human disparity representation.

A continuing area of interest concerning human stereoscopic representations is the type of disparity encoded (see Howard and Rogers 1995). These include positional disparities (eg Richards 1971; Marr 1982), spatial derivatives of disparity, such as disparity gradient (Burt and Julesz 1980) and disparity curvature (Rogers and Cagenello 1989), spatial-frequency disparity (Tyler 1975), and more recently various forms of deformation disparity (Koenderink 1986; Gillam and Rogers 1991). An early candidate representation was put forward by Wheatstone (1838), who proposed that human stereopsis used a range-mapping strategy. Such a scheme assumed the encoding of *point positional disparities*, via vergence-angle measurements taken over successive fixations. Range mapping, however, was discredited after it was shown that full stereoscopic depth could be obtained from a single fixation. Nevertheless, classical studies of human disparity representation have typically assumed an analysis of the point positional or absolute disparities in the binocular array. Studies of human stereopsis with random-dot stereograms naturally promoted a point-by-point analysis of the disparities present in random-dot targets.

Furthermore, in physiological studies of binocular cells in cats and monkeys the tendency has been to measure responses to targets containing a single value of disparity (eg Poggio and Fischer 1977). Poggio and Fischer proposed a model of 'near', 'far', and 'tuned' binocular cells responsive to positional disparities referenced to the fixation plane. Psychophysical studies have also assumed the representation of point positional disparities. Recent models, though differing in detail and sophistication from the earlier prototypes, have nevertheless postulated channels tuned to positional disparity (Lehky and Sejnowski 1990; Stevenson et al 1992).

Two key findings cast doubt over the representation of positional disparities in human stereoscopic vision. First, Collewijn et al (1986) showed, using stereoscopic targets with slowly oscillating disparity, that positional disparity does not act as a perceptual cue for 3-D structure. Second, the spatial configuration of disparities, as well as their individual magnitudes, influences the shape of the surface perceived (eg Anstis et al 1978). This indicates that local point disparities in the binocular array are spatially summated and suggests that 3-D shape is represented through a spatial, not a punctate, primitive. In the luminance domain, spatial derivatives are signalled by centre-surround odd and even symmetric receptive fields. The former signals the gradient and the latter the curvature. In the disparity domain, there is some evidence for the existence of stereoscopic channels tuned to different spatial rates of change of disparity (Schumer and Ganz 1979). Alternatively, binocular line orientation and curvature differences could provide a geometric means for signalling disparity gradient or curvature (Rogers and Cagenello 1989).

A second consideration is how the stereoscopic system represents the designated primitive, whether disparity or some derivative. This concerns the number of underlying channels used to encode the measured quantity, once extracted. Since biological cells are univariant, a single channel cannot disambiguate stimulus *value* from stimulus *intensity*. Thus, to avoid metamerism, a number of channels must be employed where each is selective for a different narrow range of values along the stimulus dimension. A large population of channels confers a high degree of resolution; however, using more channels than is required for a competent degree of discrimination is obviously costly in both biological and computational terms. In colour vision, for example, the number of different wavelength channels employed is offset by the informational cost of the genetic code for a cone pigment.

With the two principles in mind: (i) the type of disparity encoded, and (ii) the underlying channel organisation, I summarise in figure 1 some different models of human disparity representation explored in the present study. To distinguish the different models in figure 1, depth aftereffects following adaptation to a corrugated surface were measured in disparity planes either side of the plane of adaptation. Blakemore and Julesz (1971) showed that, after adaptation to two squares with different disparities, two subsequently viewed squares of equal disparity appeared to have unequal depth. They attributed their aftereffect to the adaptation of units tuned for positional disparities and proposed a multiple-tuned-channels model (figure 1, cell [2, 1]). Recent computational models have been based on a similar multi-channel principle (Lehky and Sejnowski 1990; Stevenson et al 1992). However, Rogers and Graham (1985) argued that several encoding schemes, including all those in figure 1, could account for the simple depth aftereffect. To distinguish between the two-channel and the multi-channel model, they assessed the direction (positive or negative) of their corrugated aftereffects using test surfaces whose peak-to-trough amplitudes ranged from smaller than to larger than the amplitude of the adapting surface. Their results showed the depth aftereffect was invariably negative: adaptation always reduced the perceived amplitude of the test corrugations. The absence of positive aftereffects within the range of values they tested indicated that disparity representation (0th, 1st, or 2nd order) is mediated by a two-channel

	Two-channel organisation	Multi-channel organisation
0th order representation	Crossed and uncrossed positional disparity detectors	Pools of disparity detectors, each sensitive to a particular value of positional disparity
1st order representation	Positive and negative disparity-gradient detectors	Pools of disparity-gradient detectors, each sensitive to a particular value of surface inclination
2nd order representation	Positive and negative disparity-curvature detectors	Pools of disparity-curvature detectors, each sensitive to a particular value of surface curvature

**Figure 1.** Some possible models of the organisation of human disparity representation.

opponent-process organisation. The multi-channel model predicts an additive depth aftereffect (ie an increase in perceived amplitude of same-phase test corrugations) when the test surface disparity is larger than that of the adapting surface—the well known ‘distance paradox’ effect.

In the present study, a technique adapted from Graham and Rogers (1982) was used to further address the different models outlined in figure 1. Model simulations of two widely cited encoding schemes are tested against the psychophysical data. First, the two-channel ‘opponent-process’ model (figure 1, cell [1, 1])—the disparity analogue of Sutherland’s (1961) model of motion direction. Second, the ‘multiple-tuned-channels’ model (figure 1, cell [2, 1]) proposed by Blakemore and Julesz (1971). Finally, the ‘localised disparity-gradient’ model, a new model of disparity representation is proposed, which I argue is both theoretically plausible, and best able to account for the psychophysical data.

## 2 General methods

A topping-up procedure adapted from Graham and Rogers (1982) was followed in the adaptation experiments. The scheme of the experiments is illustrated in the time histogram shown in figure 2. 50%-density random-dot stereograms (dot size  $\sim 2$  min of arc) were used to portray the adapt and test surfaces. A grey-level interpolation method allowed subpixel disparities to be presented. All surfaces were viewed through a circular porthole, 15 deg in diameter, which masked figural cues to the shape of the surface. Subjects adapted to a  $0.133 \text{ cycle deg}^{-1}$  corrugated surface with 10 min of arc peak-to-trough disparity. The surface presented two complete cycles on the screen. After adaptation, the adapt surface was briefly replaced by a test surface that was initially flat. The aftereffect appeared as a sinusoidally corrugated surface with opposite phase to the adapting surface. Subjects adjusted a potentiometer to null any aftereffect present, and the nulling disparity was taken as a measure of the strength of the aftereffect. The adapting corrugations could be offset from the fixation plane by 0,  $\pm 8$ ,  $\pm 12$ ,  $\pm 16$ ,  $\pm 20$ , and  $\pm 24$  min of arc so that the surfaces presented either all-crossed or all-uncrossed disparity values (where + denotes in front of and – denotes behind the plane of fixation). The flat test surface could be offset from the fixation plane by  $\pm 8$  to  $\pm 48$  min of arc and was positioned in disparity planes either side of the adapted plane. All disparities were presented within the limits of stereoscopic fusion.

Throughout the experiment, fixation was maintained in the plane of the screen by means of a fixation-lock stimulus with nonius markers. The adapting duration was randomised between 6 and 12 s so that subjects could not predict the onset of the test surface.

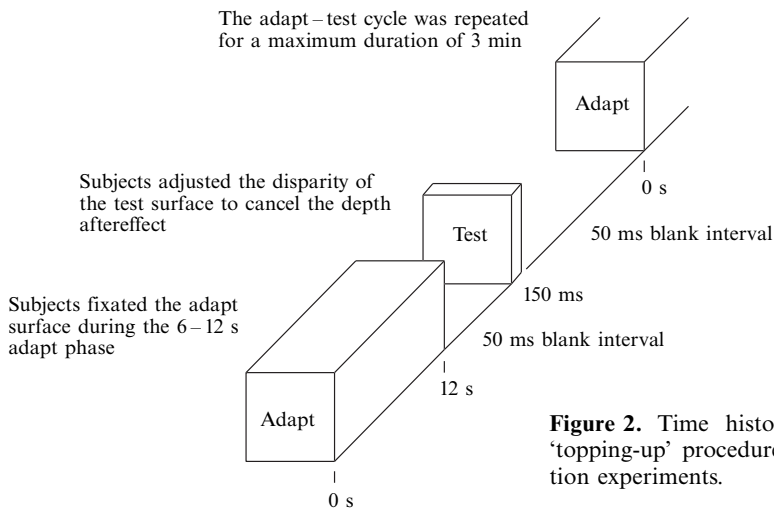


**Figure 2.** Time histogram illustrating the 'topping-up' procedure used in the adaptation experiments.

The test surface was presented briefly for 150 ms, which minimised the possibility of vergence changes during the test phase. During adaptation, subjects were required, first, to maintain correct fixation by checking the alignment of the nonius markers, and, second, to track a pixel-sized black dot (2 min of arc) which moved to and fro along a horizontal bar bisecting the 1 deg fixation spot. This procedure prevented the formation of luminance afterimages while allowing the adaptation of 'cyclopean' disparity mechanisms (Tyler 1975). The presence of any depth aftereffect was tested by a nulling procedure: Subjects adjusted a potentiometer which allowed them to add in depth to successive test surfaces to null any aftereffect present. The amount of added-in depth required to cancel the aftereffect, and make the test surface appear flat, was taken as the measure of the strength of the aftereffect. A topping-up procedure was followed in which the adapt–test cycle was repeated for a maximum duration of 3 min. Subjects were instructed not to end the trial before the 6th cycle (which was signalled by three audible beeps), and to try to establish a satisfactory match as soon as possible after the 6th cycle. This ensured a constant total adaptation time of around 1 to 1½ min in all the trials. When satisfied with a match, subjects pressed the space bar to end the trial and the matched setting was registered by the computer. There was a 1 min interval between trials. Subjects clicked the mouse button to begin the next trial.

Three participants took part in the four experiments, all with normal or corrected-to-normal eyesight. These consisted of the author plus two more psychophysical observers, one of whom was naive to the purposes of the experiment.

### 3 Adaptation experiments

#### 3.1 Experiment 1: Aftereffect adapt-disparity-plane sensitivity

In the first experiment, the aftereffect adapt sensitivity was measured: the aftereffect observed in the fixation plane as a function of adaptation to surfaces presented in near-disparity and far-disparity planes. As mentioned earlier, the psychophysical findings of Rogers and Graham (1985) suggest strongly that an opponent or *antagonistic* process operates at some level of the stereoscopic system. A very simple model might consist of two opposed channels signalling crossed versus uncrossed disparities, with the depth perceived determined by the balance of activity between these channels (cf Sutherland 1961). The present experiment was designed to distinguish between two types of disparity that may be encoded by these opponent channels. First, the two channels encode crossed

versus uncrossed *absolute disparities*, ie point magnitudes of disparity referenced to the fixation plane. Alternatively, the channels might encode *positive-disparity and negative-disparity changes* in any disparity plane, ie the fixation plane is just one of many disparity planes and does not represent a special reference point [see Howard and Rogers (1995) for a full exposition of these different types of disparity].

Adaptation to a corrugated surface in the fixation plane produces an opposite-phase aftereffect in the fixation plane (Graham and Rogers 1982). Here, we ask: if subjects adapt to a corrugated surface presented entirely in front of (or entirely behind) the fixation plane, ie surfaces presented all crossed or all uncrossed disparities, is a depth aftereffect visible in the fixation plane?

**3.1.1 Results.** Figure 3 shows the corrugated aftereffect measured in the fixation plane as a function of the adapt surface offset from the fixation plane. The aftereffect tuning function represents the mean of the results for three observers. Four observations per condition were obtained from each observer.

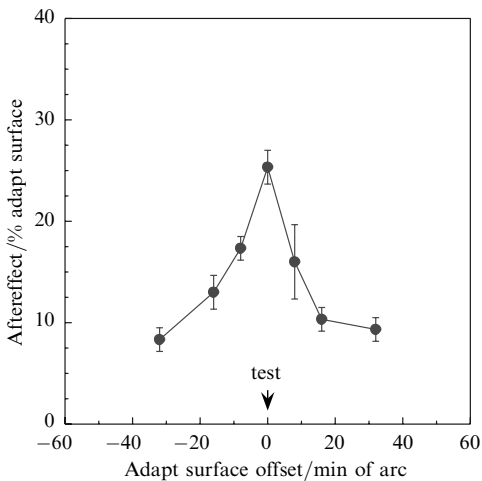


**Figure 3.** Aftereffect adapt sensitivity. Corrugated aftereffect visible in the fixation plane as a function of adaptation to surfaces presented in front of and behind the fixation plane. Each data point represents the mean of the results for three observers. The error bars show the standard errors of the means.

The depth aftereffect was always negative, ie corrugated with opposite phase to the adapting surface. The size of the aftereffect expressed as a percentage of the adapt surface amplitude is shown in the ordinate. The abscissa shows the position of the adapting surface in different trials which ranged from 32 min of arc behind to 32 min of arc in front of the fixation plane. The peak aftereffect occurred when adapt and test surfaces were positioned in the fixation plane, and ranged from 22% to 27% for the three observers. The aftereffect diminished with increasing offset of the adapting surface from the fixation plane. Thus the aftereffect exhibited a tuning characteristic with a full-bandwidth at half-amplitude of around 32 min of arc. A residual aftereffect of around 5%–10% could be observed in the fixation plane for all offsets of the adapting surface.

To check whether the tuning characteristic was due to poor fusion or attenuation of corrugations presented far from the fixation plane, two observers carried out a split-screen matching experiment. The split-screen display presented a variable-amplitude match surface in the fixation plane beside a 10 min of arc corrugated surface offset from the fixation plane in different trials by the values used in the experiments. The matched values revealed no amplitude attenuation of the corrugations presented in near-disparity or far-disparity planes. Furthermore, stereoscopic fusion was reported as effortless in all the conditions.

**3.1.2 Discussion.** A model of disparity representation based on the coding of *pure disparity changes* predicts a corrugated aftereffect irrespective of the position of the adapting surface. This is because local disparity changes in the surface (gradient or curvature) remain constant when the adapting surface is offset from the fixation plane. The result of experiment 1 rules out the coding of ‘pure disparity changes’ either by an opponent process or by multiple tuned channels, since the aftereffect varies with the plane of the adapting surface. The prediction of a model of the coding of *absolute disparities* is, in this context, less clear-cut. Initially it was supposed that such a model would predict a spike tuning function: a visible aftereffect only when adapting and testing in the same disparity plane. However, an implementation of such a model (section 4) revealed this not to be true: the absolute-disparity model produced a peak aftereffect in the fixation plane, and a gradual fall-off with increasing offset of the adapting surface—consonant with the present data. More detailed tests, however, subsequently ruled out this model. Finally, a model of disparity representation based on the coding of *localised disparity gradients*—disparity gradients within a disparity plane—is also consistent with the present result. A fuller discussion of the predictions of all three models is available with simulation data in section 4.

### 3.2 Experiment 2: Aftereffect test-disparity-plane sensitivity

In this experiment the aftereffect test sensitivity was measured: the aftereffect visible in near-disparity and far-disparity planes after adaptation in the fixation plane. The adapting surface was centred in the plane of the screen so that the peaks and troughs presented 5 min of arc crossed and 5 min of arc uncrossed disparity. This procedure, being the converse of experiment 1, yields a conventional tuning function: the effect of stimulation of one value on responses to surrounding values.

**3.2.1 Results and discussion.** Figure 4 shows the mean aftereffect test sensitivity for the same three observers. The peak aftereffect in the fixation plane,  $\sim 37\%$ , is larger than that for the identical condition in the previous experiment,  $\sim 27\%$ . This is probably due to cumulative adaptation in the present experiment owing to the repeated presentation of the adapting surface in the fixation plane. Nevertheless, the shapes of the aftereffect tuning functions for the two experiments are very similar: the bandwidth is around 27 min of arc for test sensitivity compared with 32 min of arc for adapt sensitivity. The near-identity of adapt-sensitivity and test-sensitivity tuning functions indicates that depth aftereffects reflect the adaptation of individual channels—a psychophysical principle developed by Stiles (1978), studying colour vision, to demonstrate the existence of individual channels tuned to wavelength.

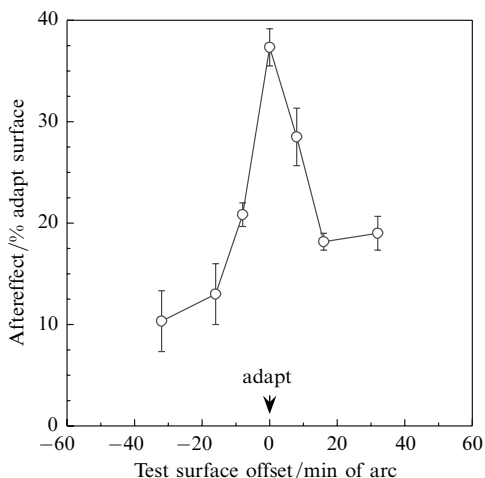


**Figure 4.** Aftereffect test sensitivity. Corrugated aftereffect visible in front of and behind the fixation plane following adaptation to a surface presented in the fixation plane. Each data point represents the mean of the results for three observers. The error bars show the standard errors of the means.

There were no significant anomalies in the appearances of the surfaces or in the nulling task. Observers reported that they could perform the nulling task with confidence even with test surfaces presented far from the plane of fixation. Where test surfaces were presented very far from the fixation plane (32 min of arc), observers reported occasionally that they could not completely flatten the test surface, and that it remained 'slightly bumpy' whichever way they turned the paddle. This suggests an adaptation nonlinearity for large offsets from the fixation plane with the peaks and troughs of the corrugated surface causing differential adaptation. This feature of the data emerges in model simulations. Nonlinear effects far from the fixation plane were also reported by Badcock and Schor (1985).

The results of experiments 1 and 2 provide further distinguishing evidence regarding the two-channel and multi-channel models. The depth aftereffects observed were always negative: *opposite-phase* compared with the adapting surface. Positive or *same-phase* aftereffects were never observed. A multi-channel model coding absolute disparities (Blakemore and Julesz 1971; Marr 1982) predicts a 'distance paradox' effect of same-phase aftereffects for certain adapt and test surface disparities. Figure 5 graphically illustrates this prediction that was not borne out by the psychophysical data. Simulation data confirm these theoretical predictions (section 4).

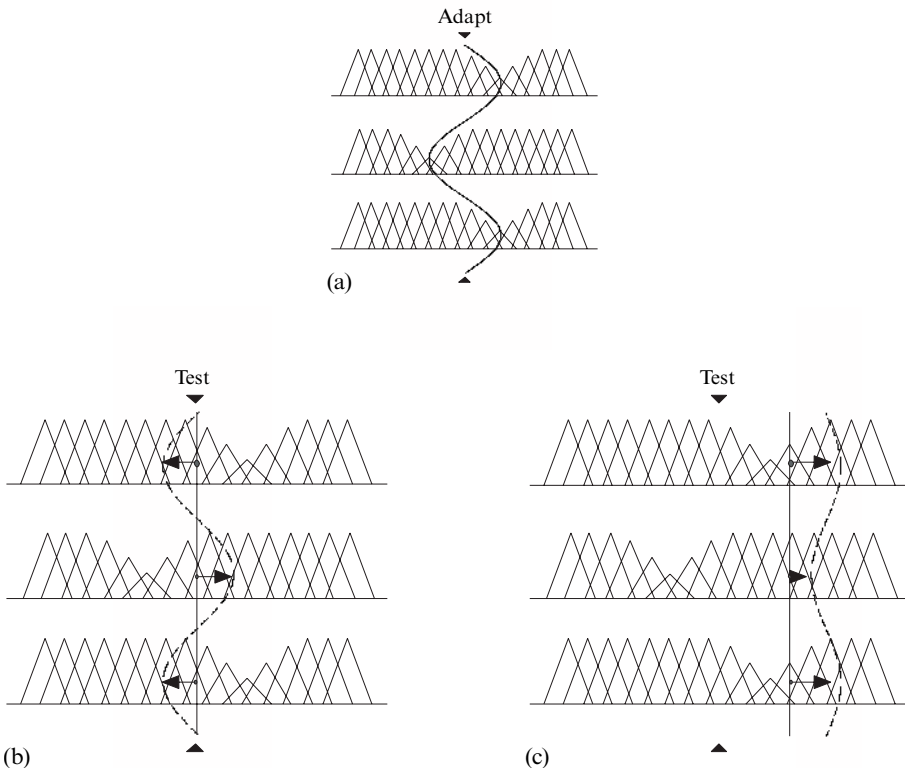


**Figure 5.** Adaptation profiles and resultant opposite-phase and same-phase aftereffect surfaces predicted by the multi-channel absolute-disparity model following the different adapt-test regimes of experiment 2. The zero-disparity (fixation) plane is indicated by the black triangular markers. (a) Adaptation profiles resulting from a corrugated adapt surface positioned in the fixation plane. (b) A flat test surface positioned in the fixation plane: the resultant centroid shifts away from the site of adaptation, indicated by the arrows, predict an *opposite-phase aftereffect*. (c) When the test surface is positioned in a different-disparity plane from that of the adapt surface, the model predicts a *same-phase aftereffect*. This is illustrated in the diagram by the centroid shifts, which are greater for test disparities near (but not in) the region of adaptation, compared with those far away. These theoretical predictions are confirmed by the simulation data.

### 3.3 Experiment 3: 'Near', 'far', and 'tuned' mechanisms?

Do the tuning functions of experiments 1 and 2 reveal a special property of the fixation plane, or are aftereffects in general tuned around the plane of the adapting surface? This question is addressed by the present experiment. The tuning functions determined so far may reflect the adaptation profile of a single mechanism (such as an opponent process) centred at the fixation plane. Such a mechanism, irrespective of which type of disparity it encoded, could account for the aftereffect tuning in the following way. First, adapt-disparity-plane tuning is the result of suboptimal adaptation when the adapting surface is offset from the fixation plane—where the mechanism is centred. Second, test-disparity-plane tuning is explained by a simple distance law of the adaptation response as the test surface is removed from the site of adaptation. These accounts accord a special status to the fixation plane. Alternatively, the fixation plane may have no special status relative to other disparity planes and aftereffects could, in general, be tuned around the plane of the adapting surface. Experiment 3 distinguished these two possibilities by presenting both adapt *and* test surfaces off the fixation plane.

**3.3.1 Results.** Tuning functions for adapting surfaces positioned 16 min of arc behind and 16 min of arc in front of the fixation plane, for the same three observers, are shown in figure 6. The middle tuning function determined in the previous experiment is also shown. In all cases the flat test surfaces were positioned either side of the adapting surface, as shown on the abscissa. Each tuning function was determined in a separate experimental session.

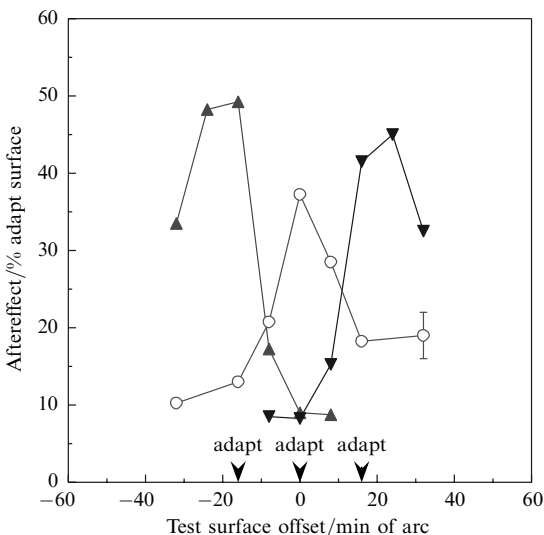


**Figure 6.** Aftereffect tuning functions for adapting surfaces positioned in  $-16$  min of arc (upright triangles) and  $+16$  min of arc (inverted triangles) disparity planes. The  $0$  min of arc tuning function determined in experiment 2 is also shown (open circles). Each data point represents the mean of the results for three observers. The error bar shows the average standard error of the means.

**3.3.2 'Near', 'far', and 'tuned' disparity detectors?** The results indicate that tuning functions can be established off the fixation plane and that aftereffects are tuned around the plane of the adapting surface. The magnitudes of the peak aftereffects for  $\pm 16$  min of arc tuning functions were around 50% larger than the peak aftereffects in the fixation plane. All three tuning functions have similar bandwidths (around 24 to 32 min of arc). Note that the peaks of both crossed and uncrossed tuning functions are shifted slightly farther away from the fixation plane compared with the plane of the adapting surface. These results are reminiscent of a particular model of disparity representation in which just three channels are postulated sensitive to near and far disparities and disparities around the fixation plane (Richards 1971). Early electrophysiological studies appeared also to indicate that disparity-sensitive neurons in the cat could be divided into three broad categories of 'near', 'far', and 'tuned' cells (Poggio and Fischer 1977). The three tuning



curves could therefore reflect the response profiles of the three postulated mechanisms. This hypothesis is addressed in the final experiment.

### 3.4 Experiment 4: Multiple tuned channels?

Experiment 4 addresses the question whether the aftereffect tuning functions of figure 6 reflect the response profiles of just three underlying pools of disparity detectors (Richards 1971), or whether they correspond to just three of a potentially much larger set of possible tuning functions. Stevenson et al (1992) have argued that the number of distinct adaptation profiles provides an indication of the minimum number of underlying channels. If the representation of disparity is mediated by only a small number of broadly tuned mechanisms, irrespective of whether these are 0th order detectors (eg Richards 1971) or localised 1st or 2nd order detectors, then aftereffect tuning profiles for different disparity planes of adaptation should peak at or close to the peak sensitivity of the nearest underlying channel, perhaps near 0 and  $\pm 16$  min of arc. On the other hand, if multiple tuned mechanisms underlie disparity representation, then the aftereffect should be tuned around the disparity plane of the adapting surface.

**3.4.1 Results.** Aftereffect tuning functions were determined for several different disparity planes of the adapting surface in both crossed and uncrossed directions. Each tuning function was determined in a separate experimental session, though they are shown together in figure 7. The bandwidths of the tuning functions range from 16 to 32 min of arc. The peaks of the aftereffect profiles do not appear to coincide with the peak sensitivities of just three underlying channels. Selective adaptation occurred such that the peak aftereffect was observed at or near to the plane of the adapting surface. The magnitudes of the peaks of the tuning functions increased with increasing offset of the adapt surface from the fixation plane. When adapt and test surfaces were presented far from the fixation plane, the peaks of the resulting tuning functions were shifted even farther away from the fixation plane than the plane of the adapting surface. Finally, the shapes of the tuning functions exhibit a marked asymmetry, with the near side of the curve to the fixation plane being steeper than the far side. These properties of the data were used to evaluate the simulations in the next section.

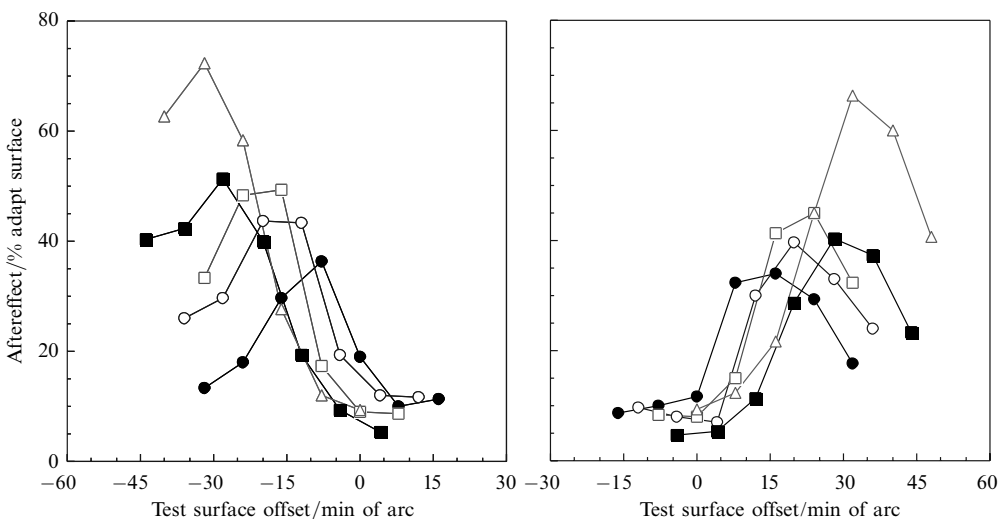


**Figure 7.** Crossed-disparity (right) and uncrossed-disparity (left) aftereffect tuning functions. The adapting surfaces were positioned in  $\pm 8$  (solid circles),  $\pm 12$  (open circles),  $\pm 16$  (open squares),  $\pm 20$  (solid squares), and  $\pm 24$  (open triangles) min of arc disparity planes. Each data point represents the mean of the results for three observers.

## 4 Model simulations

The properties of the aftereffects determined in experiments 1 through 4 were used to evaluate three different models of disparity representation: (i) the classical opponent-process model (Sutherland 1961); (ii) the classical multiple-tuned-channels model (Marr 1982); and (iii) a localised disparity-gradient model—a new model proposed in the present study. The models were implemented on a Unix Sun work station, each one providing a full data set corresponding to the experiments. For the sake of brevity, only selected data plots are presented where they critically bear on the arguments advanced.

### 4.1 General modelling techniques

Model channels and corrugated stimuli were represented by means of pre-computed arrays which served as stimulus and response look-up tables during the simulation runs. HIPS (Heritable Image Processing Software) was used to create the arrays and to display them in the grey-level domain. Since the corrugated stimulus varied in one direction only—sinusoidal in the vertical direction—the stimulus was represented adequately with a one-dimensional array of size 1 pixel  $\times$  256 pixels which accommodated the two complete cycles of the corrugated surface. The channels were represented with a two-dimensional array of size 256 pixels  $\times$  256 pixels. The array consisted of 256 individual channel profiles, each 'looking at' a different horizontal raster of the corrugated surface. Within a single-channel array, the array *number* represented the stimulus dimension: either disparity or disparity gradient, depending on the particular model implemented. The array *value* represented the channel's response to the stimulus. Disparity tuning could be effected by shifting the whole profile by the desired value along the channel array. In practice, the stimulus array was shifted instead of the channel arrays. This manoeuvre saved computation time by allowing an arbitrarily large number of channels to be implemented, on the basis of a single pre-computed prototype.

Adaptation was modelled by computing new arrays to represent responses of the adapted channels. The adapted arrays provided new look-up values for the test surface and resultant aftereffect surface. Adaptation was directly proportional to stimulation, and the gain of adaptation could be controlled by adjusting a single parameter which set the overall adaptability of the channel. Details of the input–output calculations for the individual model simulations are provided with the simulation data below.

### 4.2 Opponent-process model

The simplest model of human disparity representation that has been proposed is a *two-channel opponent-process model* signalling cross and uncrossed disparities. This is the disparity analogue of the two-channel model of motion direction proposed by Sutherland (1961). Perceived depth is determined by the balance of activity between two channels broadly tuned to crossed and uncrossed disparities. In the following implementation, Gaussians were used to model the responses of the opponent channels. The Gaussians were centred at  $\pm 8$  min of arc disparity and the standard deviation was set to  $\sigma = 32$  min of arc. The output was obtained by taking the algebraic difference between the two Gaussians, so that effectively a difference-of-two-Gaussians (DOG) filter was applied to the input surface. Adaptation was modelled by attenuating the Gaussians in proportion to the look-up value obtained from the adapt surface, and applying the attenuated Gaussians to the test surface. The gain of adaptation was calibrated with the psychophysical data.

The simulation data (figure 8) exhibited the following characteristics: Aftereffect adapt and test sensitivity functions (experiments 1 and 2) had markedly different tuning bandwidths with test sensitivity being much broader than adapt sensitivity. This occurred because the most effective adaptation was always produced by an adapting surface in the fixation plane which stimulated the opponent channels most effectively.

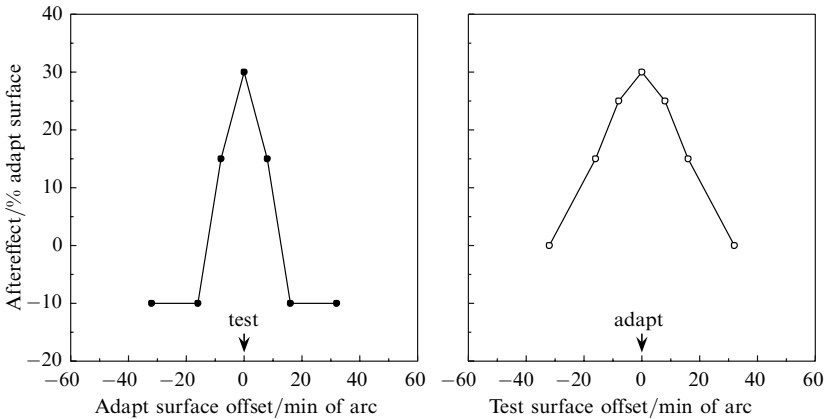


**Figure 8.** Simulation data for experiments 1 and 2 produced by an implementation of the opponent-process absolute-disparity model. The model predicts markedly different adapt-disparity-plane (left) versus test-disparity-plane (right) sensitivity functions, in contrast to the psychophysical data in which the two profiles are very similar (see figures 3 and 4). Furthermore, the model predicts a phase reversal of the aftereffect surface under certain conditions as indicated by the negative aftereffect values in the left panel.

In addition, selective adaptation was not observed after adaptation in different disparity planes (experiments 3 and 4). All tuning functions peaked in the fixation plane, unlike the human data in which different aftereffect tuning functions could be established for the different disparity planes of adaptation. The largest aftereffects occurred when the adapting surface was positioned near to the fixation plane, in contrast to the human data in which the reverse was observed—largest aftereffects were obtained for adaptation far from the fixation plane (data plots not shown). Therefore the simulation results failed to capture significant properties of the human data, and the opponent-process model of positional disparity representation was rejected.

### 4.3 Multiple-tuned-channels model

The next simulation is of a multi-channel model of the coding of absolute disparities. The multi-channel organisation operates on the principle of *labelled line* or *place* coding. The response of each channel signifies a particular value on the dimension, and the magnitude of the response signifies the probability of that value. The total population activity is therefore a probability distribution from which the mean, or expected value, can be extracted. This principle differs from the opponent-process organisation of the previous model where the channels are broad and overlapping, do not label a particular quantity but simply a *sign* on a bipolar dimension, and the response magnitude is a graded variable indicating the magnitude of the stimulus sign. Gaussian response profiles were used to represent the channels. The centroid of the channel population was taken as the output disparity. Different simulation runs explored the effects of (i) channel population size  $N$ ; and (ii) channel bandwidth  $\sigma$ .

Unlike the opponent-process model, the multi-channel model produced disparity-plane-selective adaptation to varying degrees depending on the underlying channel structure. When the channel population was small ( $N = 5$ ), the tuning functions peaked near the region of the closest underlying channel. When  $N = 9$ , the tuning functions began to exhibit some differentiation (see figure 9).

Increasing the bandwidths of the channels with a fixed population size had a similar effect as increasing the population size for a fixed channel bandwidth. Both manipulations increase the overlap between channel profiles, which leads to a distributed representation of the stimulus. However, the model predicts a phase reversal of the aftereffect surface, producing same-phase aftereffects for certain distances between

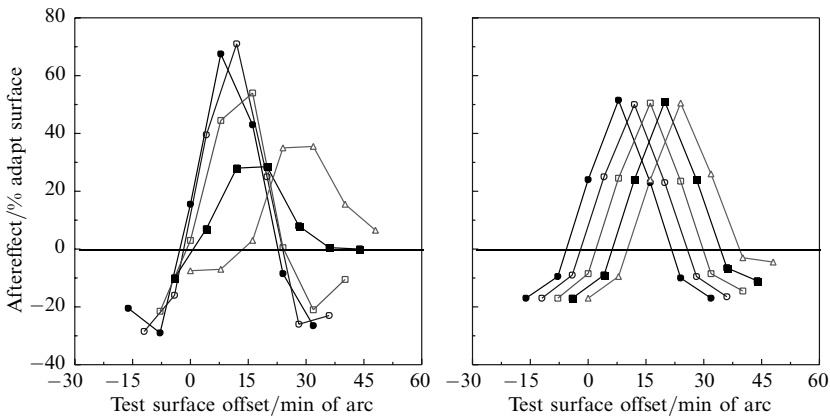


**Figure 9.** Simulation data produced by two implementations of the multi-channel absolute-disparity model. Data on the left were produced by a population of 5 underlying channels, and on the right by 9 channels. The channel bandwidth was fixed at  $\sigma = 16$  min of arc. Increasing the population size led to selective adaptation and differentiation of the tuning functions. Increasing the channel bandwidth for a given population size had a similar effect. The negative values below the dashed line signify a phase reversal of the aftereffect surface i.e. a predicted same-phase aftereffect.

adapt and test surface disparities—confirming previous theoretical arguments. As mentioned previously, same-phase aftereffects were never observed by subjects in any of the experiments. Consequently the generic multiple-tuned-channels model of the coding of absolute disparities was rejected.

#### 4.4 Localised disparity-gradient model

The final model presented is based on the coding of disparity gradients by disparity-plane localised channels. The response of each channel is determined by (i) Gaussian weighting over disparity, and (ii) difference-of-Gaussian (DOG) weighting over disparity gradient. Figure 10 shows a plot of the 2-D weighting function of a single channel.

The channel codes positive and negative disparity gradient within a preferred disparity plane. The model therefore presumes the extraction of a different primitive compared with the previous models. In the simulations, the front-end extraction of disparity gradient was not modelled but assumed—disparity gradients were pre-calculated and input to the model. In different simulation runs, the effects of channel bandwidth and

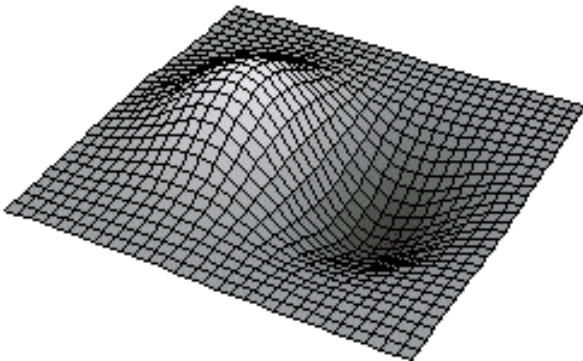


**Figure 10.** Response profile of a single channel comprising the localised disparity-gradient model. The 2-D weighting function is Gaussian over disparity and difference-of-Gaussian over disparity gradient. In simulations, a variable number of such channels tuned to different disparity planes could be specified.

population size were explored. As in the previous simulations, disparity-plane-selective adaptation was dependent on channel population size and the degree of overlap between channel profiles. Figure 11 shows results of a simulation in which  $N = 7$  and  $\sigma = 24$  min of arc. In addition, the adaptability parameter  $\beta$  of individual channels was scaled according to a power function of the channel offset from the fixation plane, as suggested by the experimental data.

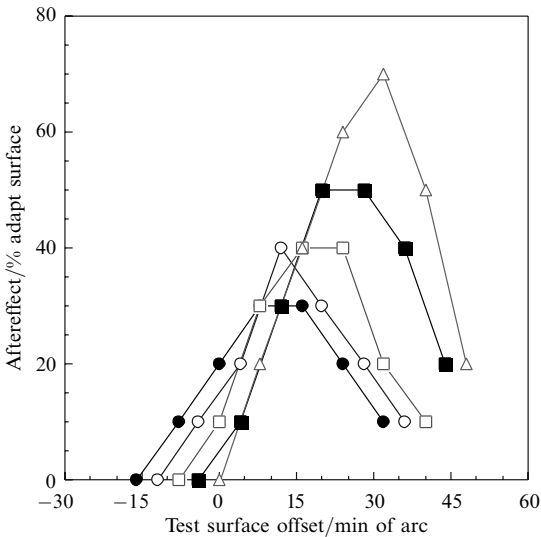


**Figure 11.** Model tuning functions resulting from a simulation of the localised disparity-gradient model. In the above simulation run, 7 channels encoding positive versus negative disparity gradient were localised at equal disparity intervals from  $-64$  to  $+64$  min of arc. The channels had identical bandwidths ( $\sigma = 24$  min of arc) and channel adaptability was scaled according to a power function of distance from the fixation plane.

Only crossed-disparity tuning functions are shown since uncrossed-disparity tuning functions are simply mirror reverse. The simulation data can be compared with the observer data of figure 7 (right panel). The model is not a perfect simulation of the psychophysical data. However, the following significant characteristics are displayed; peak aftereffects increase as a power function of the adapt surface offset; for large adapt and test disparities, the peaks of the tuning functions are shifted around 4 min of arc even farther from the fixation plane than the plane of the adapting surface; the shapes of the tuning functions are asymmetric about the peak value with the near-side of the tuning curve to the fixation plane steeper than the far-side. Furthermore, though not shown, the simulation tuning functions for aftereffect adapt and test sensitivity were identical—as indicated by the human data. The human data, however, show a flattening-off of the tuning functions as they move towards asymptote for far in-front-of test surfaces. This feature is not displayed by the simulation data. It is reminiscent of lateral inhibition which was not built into the model. It is not clear, however, why there should be a difference between far in-front-of and far behind plane effects.

The localised disparity-gradient model produced tuning functions which simulated some significant features of the human data. On the basis of these results, I propose that the underlying structure of human disparity representation may be organised on a similar principle.

## 5 Conclusion

In section 3 an adaptation method was used to examine the structure of human disparity representation. Aftereffect tuning functions were used in section 4 to evaluate three candidate models of disparity representation. Two of these—the opponent-process model and the multiple-tuned-channels model—are frequently cited in the literature. Neither model performed satisfactorily in the simulations. A localised disparity-gradient model was developed to account for the adaptation data. An implementation of this model

yielded results which simulated the human data in many respects. In addition to the present findings, there is a wealth of evidence from other sources to suggest the representation of disparity changes by human stereo mechanisms. The present data reveal that a pure disparity-change mechanism (either gradient or curvature) does not apply in the case of human observers: depth aftereffects are selectively tuned around the plane of the adapting surface. This suggests that the channels coding disparity changes are localised within disparity planes. From a biological point of view this would be most likely, since a disparity-gradient operator necessarily receives its input, initially, from receptors coding retinal local sign differences, ie positional disparities. Different sets of such cells would be activated by adapting surfaces presented in different disparity planes. I suggest therefore that disparity change is the primary code and that the channels carrying these codes are localised within disparity planes.

Why, as the data and model suggest, should channels located far from the fixation plane be more adaptable than those located close to the fixation plane? Perhaps the different adaptabilities of the channels reflect differences in image statistics for objects viewed in and out of the fixation plane? According to the statistical theory of adaptation (Watt 1988), a perceived value of, say, curvature is defined in relative, not absolute, terms. Thus, under normal viewing conditions, the distribution of convex and concave curvatures is symmetrical and equal about a midpoint—which comes to define perceived flatness. Prolonged exposure to one value skews the distribution and shifts the midpoint. The resulting adaptation or recalibration defines a new value as the midpoint of curvature—thus a curved surface is perceived as flat. The greater adaptability of channels off the fixation plane suggests that image statistics, or their encoding, may be less stable for objects not fixated. However, we cannot as yet explain this feature of stereoscopic processing off the plane of fixation.

**Acknowledgements.** I thank Brian Rogers, Andrew Glennerster, and Richard Eagle for the useful discussions while this work was being carried out; Peter Caryl and Ian Deary for comments on a draft manuscript; and finally the reviewers for their observations.

## References

- Anstis S M, Howard I P, Rogers B J, 1978 "A Craik–O'Brien–Cornsweet illusion for visual depth" *Vision Research* **18** 213–217
- Badcock D R, Schor C M, 1985 "Depth increment detection functions for individual spatial channels" *Journal of the Optical Society of America A* **2** 1211–1215
- Blakemore C, Hague B, 1972 "Evidence for disparity detecting neurones in the human visual system" *Journal of Physiology (London)* **225** 437–455
- Blakemore C, Julesz B, 1971 "Stereoscopic depth aftereffects produced without monocular cues" *Science* **171** 286–288
- Burt P, Julesz B, 1980 "A disparity gradient limit for binocular fusion" *Science* **208** 615–617
- Collewijn H, Erkelens C J, Regan D, 1986 "Absolute and relative disparity: a re-evaluation of their significance in perception and oculomotor control", in *Adaptive Processes in Visual and Oculomotor Systems* Eds E L Keller, D S Zee (Oxford: Pergamon Press) pp 177–184
- Gillam B, Rogers B J, 1991 "Orientation disparity, deformation, and stereoscopic slant perception" *Perception* **20** 441–448
- Gillam B, Ryan C, 1992 "Stereoscopic after-effect determined by disparity gradient" *Investigative Ophthalmology & Visual Science* **33**(4) 1371
- Graham M E, Rogers B J, 1982 "Simultaneous and successive contrast effects in the perception of depth from motion-parallax and stereoscopic information" *Perception* **11** 247–262
- Howard I P, Rogers B J, 1995 *Binocular Vision and Stereopsis* (Oxford: Oxford University Press)
- Koenderink J J, 1986 "Optic flow" *Vision Research* **26** 161–180
- Lehky S R, Sejnowski T J, 1990 "Neural model of stereoacuity and depth interpolation based on a distributed representation of stereo disparity" *Journal of Neuroscience* **10** 2281–2299
- Marr D, 1982 *Vision: A Computational Investigation into the Human Representation and Processing of Visual Information* (San Francisco, CA: W H Freeman)
- Poggio G F, Fischer B, 1977 "Binocular interaction and depth sensitivity in striate and prestriate cortex of behaving rhesus monkey" *Journal of Neurophysiology* **40** 1392–1405

- 
- Richards W, 1971 "Anomalous stereoscopic depth perception" *Journal of the Optical Society of America* **61** 410–414
- Rogers B J, Cagenello R B, 1989 "Disparity curvature and the perception of three-dimensional surfaces" *Nature (London)* **339** 135–137
- Rogers B J, Graham M E, 1985 "Motion parallax and the perception of three-dimensional surfaces", in *Brain Mechanisms and Spatial Vision* Eds D J Ingle, M Jeannerod, D N Lee (Dordrecht: Martinus Nijhoff)
- Schumer R A, Ganz L, 1979 "Independent stereoscopic channels for different extents of spatial pooling" *Vision Research* **19** 1303–1314
- Stevenson S B, Cormack L K, Schor C M, Tyler C W, 1992 "Disparity tuning in mechanisms of human stereopsis" *Vision Research* **32** 1685–1694
- Stiles W S, 1978 *Mechanisms of Colour Vision* (London: Academic Press)
- Sutherland N S, 1961 "Figural aftereffects and apparent size" *Quarterly Journal of Experimental Psychology* **13** 222–228
- Tyler C W, 1975 "Stereoscopic tilt and size aftereffects" *Perception* **4** 187–192
- Watt R J, 1988 *Visual Processing: Computational, Psychophysical and Cognitive Research* (Hillsdale, NJ: Lawrence Erlbaum Associates)
- Wheatstone C, 1838 "Contributions to the physiology of vision. Part the first. On some remarkable, and hitherto unobserved phenomena of binocular vision" *Philosophical Transactions of the Royal Society of London* **128** 371–394

